

AN EXPERIMENTAL STUDY ON THE TSUNAMI BOULDER MOVEMENT

Haijiang Liu¹, Taiki Sakashita², and Shinji Sato²

A number of displaced tsunami boulders were observed through the subsequent in-site surveys after the 2011 Tohoku tsunami event. In this study, a series of dam-break type hydraulic experiments were carried out in an open channel with a concrete block setting on a horizontal bed just above the beach face to simulate the tsunami-induced boulder overland movement process. Three different initial water head settings were applied with three different tsunami-boulder interaction angles. Instantaneous water level and bore current velocity were measured, and the entire boulder moving process was recorded using a video camera. Sliding boulder movement was observed in the experiments. Comparing to the normal incident tsunami, oblique incoming tsunami wave resulted in a longer boulder displacement owing to the larger current-projected area. It was confirmed that the block dislodgement is not triggered immediately by the arriving of the water bore, but there exists a measurable time lag between the tsunami arrival and the inception of boulder movement. A small difference in the initial water head settings could lead to a significant difference on the total boulder displacement. As for the boulder moving process, three phases were identified from the experiment, i.e., the acceleration phase (at the beginning stage), the deceleration phase (in the middle stage), and the relatively steady moving phase (in the end). From the experiment, it was confirmed that the difference in the total boulder displacement is mainly ascribed to the boulder moving velocity difference during the deceleration and steady moving phases.

Keywords: Tsunami boulder; Dam-break hydraulic experiment; Bore velocity; Boulder moving process; Boulder displacement; Boulder velocity

INTRODUCTION

Coastal boulders are good evidence of tsunami attack, which is an extremely high energy event capable of displacing, transporting and emplacing huge and heavy loads a few to several hundred meters away from their original locations. Such tsunami boulder movement has been reported worldwide, such as in Okinawa, Japan (Kato and Kimura, 1983), along southeastern and western coasts of Australia (Bryant et al., 1992; Nott and Bryant, 2003), in Flores, Indonesia (Shi et al., 1995), in Ionian, Italy (Mastronuzzi and Sansò, 2000; Scicchitano et al., 2007), in Portugal (Costa et al., 2011) and in Hawaii (Goff et al., 2006). Dawson and Shi (2000), Scheffers and Kelletat (2003) presented general reviews on different tsunami imprints, together with their geomorphological and sedimentological characteristics. Huge erratic boulders transported by the prehistoric tsunamis have also been reported in Bahamas with a volume/weight about 1000 m³/2300 tons (Hearty, 1997), and in Tonga with a volume/weight about 780 m³/1600 tons (Frohlich et al., 2009). Since the 2004 Indian Ocean modern tsunami event, the boulder transport has been further investigated through detailed post-tsunami field surveys (Razzhigaeva et al., 2006; Goto et al., 2007; Paris et al., 2010; Etienne et al., 2011).

In the immediate aftermath of the 2011 Tohoku earthquake tsunami, a number of displaced tsunami boulders were confirmed through the subsequent field surveys. Figure 1 shows two typical tsunami boulders observed during our post-tsunami surveys in Fukushima and Iwate Prefecture, respectively. These huge and heavy objects were entrained from their original locations and deposited inland by the powerful tsunami flows. The concrete seawall block in Fig. 1(a) was displaced from its construction foundation and moved landward by 35 m with a 5 m local flow depth measured in our field survey. The overturned boulder in Fig. 1(b) was transported about 30 m inland from its initial position with a 14 m local tsunami flow depth (Liu et al., 2013). This boulder was supposed to move further landward if there was no impediment from the behind building (Fig. 1b).

Investigation on such boulder movement provides valuable information to help identify and interpret palaeo-tsunami imprints on the coastal landscapes, which could be used to estimate the nature and behavior of these extreme events and be useful for evaluating the risk of future tsunami disasters and aiding in future disaster mitigation efforts (Imamura et al., 2008; Pignatelli et al., 2009; Etienne et al., 2011). To understand the boulder transport processes, a large quantity of studies was conducted on the basis of field investigations looking at boulder spatial distribution and accumulation feature, boulder size, weight and orientation, the surrounding lithology and morphology to indicate boulder geographic

¹Corresponding author. Ocean College, Zhejiang University, 866 Yuhangtang Road, Hangzhou, Zhejiang, 310058, China. haijiangliu@zju.edu.cn.

²Department of Civil Engineering, the University of Tokyo, 7-3-1 Hongo, Bunkyo-ku, Tokyo 113-8656, Japan.

origin and physiographic setting (aforementioned references). Although field surveys provide significant first-hand information, interpretation on boulder-related outcomes is subtle due to the many unknown, unclear or uncontrollable field conditions, e.g., waves characteristics (height and current velocity), local landform features (roughness and microtopography) and boulder irregularities (size and density, as well as the inter-granular collision during transport). Consequently, some field-based research results remains controversial (Scheffers et al., 2009; Hall et al., 2010; Switzer and Burston, 2010; Etienne et al., 2011).



Figure 1. Relocated tsunami boulders observed in the 2011 Tohoku earthquake tsunami field survey. (a) A relocated concrete seawall block (0.5×1.6×2.24×10 m in size with an estimated weight about 56 ton) in Nakoso, Fukushima Prefecture (Sato et al., 2012). (b) An overturned boulder sitting in front of the city arena (2.0×2.1×3.6 m in size with an estimated weight about 38 ton) in Rikuzentakata, Iwate Prefecture. (Liu et al., 2013)

On the other hand, laboratory experiments could be applied to understand the fundamental mechanism controlling boulder dislodgement, emplacement and transport under designed tsunami conditions. However, to our knowledge, only a few experiments were reported in the literature. Noji et al. (1993) performed hydraulic experiments in a horizontal channel using breaking bores to formulate the drag and mass coefficients. Later, Imamura et al. (2008) carried out experiments using a tsunami water tank with cubic and rectangular shaped blocks on the slope to investigate the boulder transport process. At the same time, numerical models were developed to figure out various hydraulic properties related to boulder moving processes, such as the inundation depth, current velocity and hydraulic forces. Nott (2003) developed hydrodynamic equations to assess the boulder movement theoretically for different initial positions, such as submerged, subaerial and joint-bounded. Similarly, Noormets et al. (2004) theoretically estimated boulder dislodgment, emplacement and transport processes. Pignatelli et al. (2009) developed a simple relationship to find the transport distance of a boulder based on Nott's equations. Recently, Nandasena et al. (2011) revised Nott's 2003 equations and showed a better estimation on velocity from field survey. However, the results of Nott's equations should be applied with caution (Hall et al., 2010; Switzer and Burston, 2010; Nandasena et al., 2011). Based on Noji et al. (1993), Imamura et al. (2008) on the other hand proposed a practical model for boulder transport by tsunamis, which takes into account various transport modes, such as sliding, rolling and saltation. Goto et al. (2010) then applied this model to the boulder transport in the 2004 Indian Ocean tsunami at Pakarang Cape, Thailand. They showed that boulder movement is strongly controlled by the local topography, tsunami hydrodynamic features and the initial distribution of boulders at the source.

In this study, considering field observations following the 2011 Tohoku earthquake tsunami, hydraulic experiments were carried out in an open channel with a rectangular shaped concrete block on a horizontal bed just above the beach face to simulate the boulder overland transport process induced by tsunamis. Physical insights of the boulder moving characteristics were revealed from experimental studies. In the following context, hydraulic experiment set-up will be specified firstly, followed by the measurement results (e.g., temporal water level and current velocity), experimental interpretation, and discussions on the boulder moving process and velocity.

HYDRAULIC EXPERIMENT

Experimental Set-up

A series of laboratory experiments was conducted in a tsunami water tank at Tokyo University of Marine Science and Technology. Schematic diagram showing the water tank for hydraulic experiments is presented in Fig. 2. The total length/width of the water tank is 18 m/1 m, respectively. A tsunami bore was generated using the dam break method by releasing a volume of water in a reservoir setting at the left end of the tank with an 8 m length. This approach allows the experiments to be carried out on a larger scale with smaller scale effects (Ramsden, 1993). A gate located at 8 m from the upstream end of the tank confines water in a storage tank, and acts as a wave generator. A tsunami bore is thus generated by rapid opening of this gate. An initial water depth at the downstream side of the gate was kept as 10 cm. Comparing with a dry bed surge, applying a wet bed with a small still water depth can provide a steeper wave front for the generated turbulence bore due to the small bed surface friction (Ramsden, 1993).

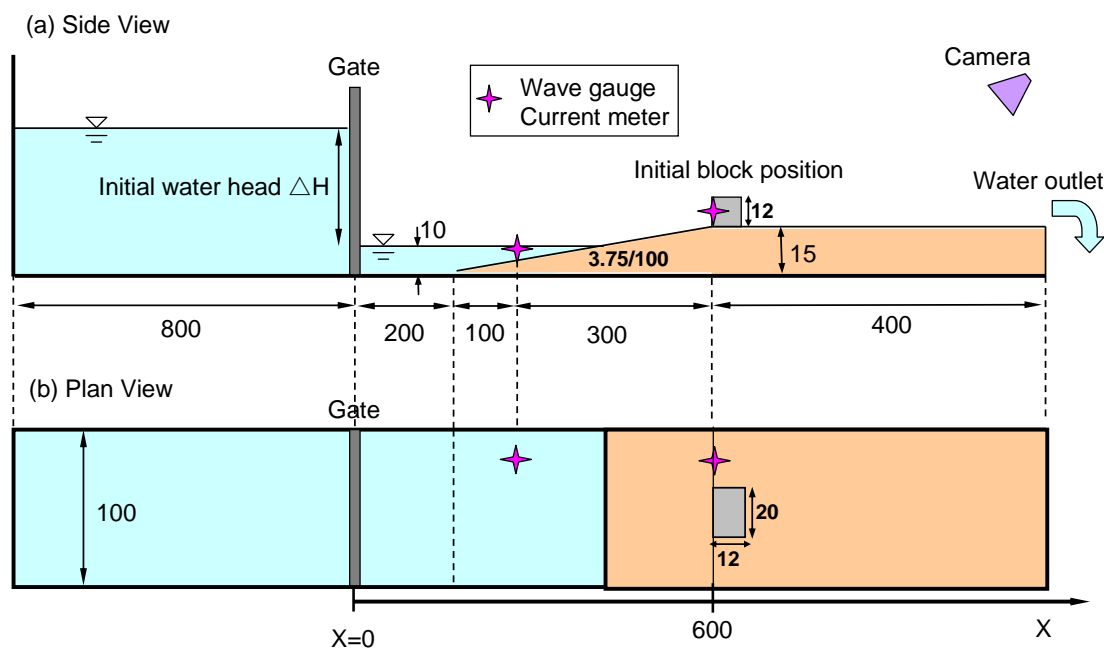


Figure 2. Schematic diagrams of the water tank for hydraulic experiments. (a) Side view (b) Plan view. All dimensions are in cm.

In this study, we were focusing on the overland tsunami boulder movement as shown in Fig. 1. In the field, these boulders were initially subaerial and located at a relatively flat terrain. Taking this into account, a flat slope followed by a horizontal plate was used which was set at 2 m downstream from the gate where the bore becomes steady and stable (Fig. 2). This setting simulates the nearshore environment representing the subaqueous and terrestrial landform. The gradient of the slope was 3.75:100. The wooden slope and plate were smooth and impermeable. The generated bore runs up the slope, flushes through the horizontal plate and outflows from the other end of the channel. A rectangular shaped concrete block with a size 12×12×20 cm and a density 2.4 g/cm³ was placed at the beginning of the horizontal plate to mimic the field condition. Considering that tsunamis may attack boulders with an oblique angle in the field, except the perpendicular incidence of tsunami with respect to the long axis of boulders (Case I), an initial setting with a tsunami-boulder (long axis) orientation of 45 (Case II) and 0 (Case III) degrees was also applied in hydraulic experiments (as shown in the schematic diagrams in Table 1). Applying this system, we can investigate the boulder movement under which the boulder is mobilized by a single bore.

The time series of the water levels and current velocities were measured using a capacitance-type wave gauge and an electromagnetic-type current meter with a sampling frequency of 50 Hz at two specified locations (Fig. 2), the middle of the slope and the initial position of the block. After a number of pretests, the water levels in the storage tank were set at 40, 42 and 45 cm for investigating the

boulder movement, corresponding to an initial water head setting of 30, 32 and 35 cm, respectively. Each hydraulic experiment was performed three times and the boulder movement process and transport path were recorded using one video camera from the ending top of the channel (Fig. 2). In the following discussion, position $x=0$ m is set at the gate with a positive value towards the channel downstream.

Temporal Water Level

Figure 3 shows the temporal variation of the measured water level at the initial block position, i.e., $x=6$ m, for three different initial water head settings (IWHS, ΔH). The turbulent bore could be clearly observed with a steep wave front, and the water level reaches its maximum value about 6 second after the bore arrival, following by a gradual decrease. In Fig. 3, it is confirmed that a larger IWHS leads to a higher temporal water level during almost the whole experimental period. The recorded maximum water level is 11.75 cm, 12.38 cm and 13.31 cm for the $\Delta H = 30$ cm, 32 cm and 35 cm, respectively, which corresponds to 39%, 39% and 38% of the IWHS, respectively. This is in agreement with the description in Ramsden (1993) experiments, who found the bore height is about 4/9 of the original water head in the reservoir. The differences on the maximum bore heights of different IWHSs are 0.63 cm ($\Delta H = 30\sim 32$ cm) and 0.93 cm ($\Delta H = 32\sim 35$ cm), which correspond to 32% and 31% of the IWHS difference, i.e., 2 cm and 3 cm respectively.

Time Series of Current Velocity

Figure 4 presents the instantaneous measured current velocity at the 3m location for three different ΔH . Considering that the electromagnetic-type current meter could not play its function under the subaerial condition, the current meter probe was deployed beneath the initial 10 cm water surface 3 m downstream of the tank gate in our experiment as shown in Fig. 2, resulting in a subaqueous environment. In Fig. 4, it is observed that there is a sudden increase of bore velocity up to around 1.3 m/s (within ~ 0.6 sec of the bore arrival) for all ΔH in our experiments. Accordingly, the flow acceleration is estimated as large as 2.3 m/s^2 . After the maximum bore velocity, the decreasing process is relatively gradual. Although the 35 cm ΔH with a large measured temporal water level in Fig. 3, in general, leads to a slightly larger velocity in the deceleration phase, there is no significant difference on the instantaneous bore velocity variation, including the maximum velocity, among the three different ΔH .

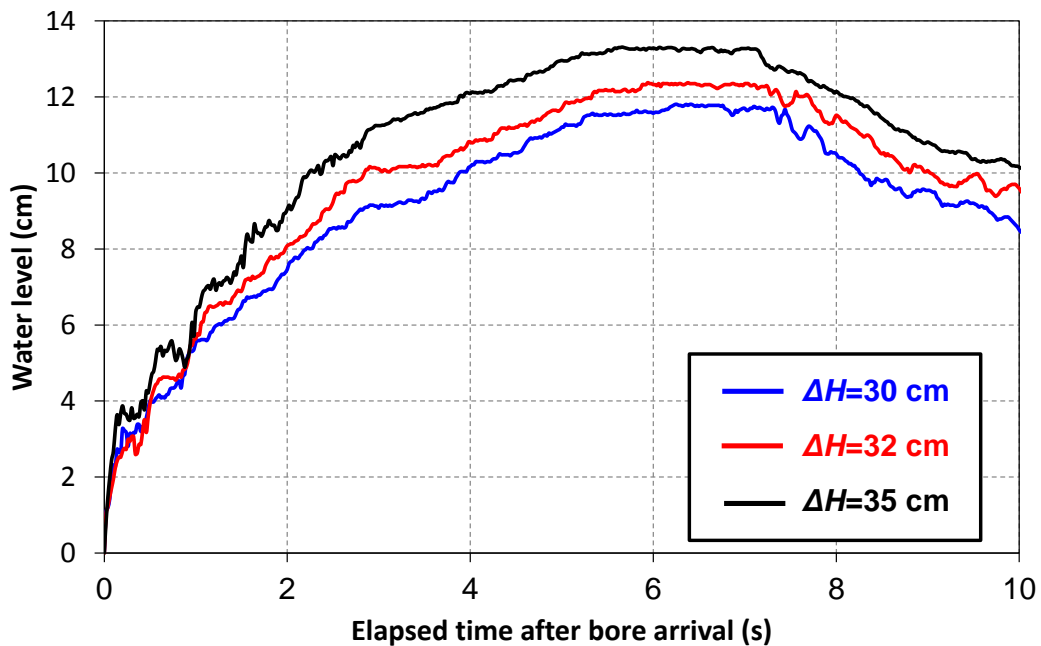


Figure 3. Temporal water level variation at the initial block position for three different ΔH .

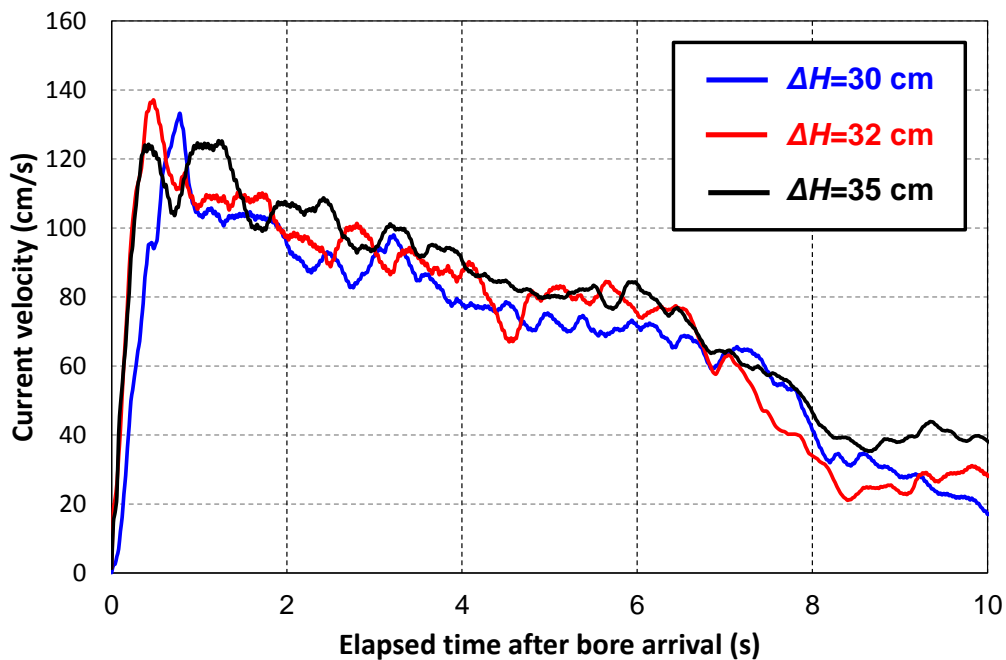
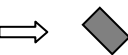


Figure 4. Measured current velocity at the 3 m location (Fig. 2) for three different ΔH .

Table 1: Measured boulder displacement for all experimental settings. Arrows and rectangles represent the flow direction and the block orientation, respectively.

		Initial water head ΔH		
		30 cm	32 cm	35 cm
Case I (90°) 	Displacement (cm)	1, 0, 0	113, 116, 115	230, 187, 235
	Average (cm)	0.3	114.7	232.5
Case II (45°) 	Displacement (cm)	6, 0, 0	130, 131, 150	229, 227, 214
	Average (cm)	2.0	137.0	223.3
Case III (0°) 	Displacement (cm)	0, 0, 0	0, 0, 0	0, 0, 0
	Average (cm)	0	0	0

: This small value is caused by the impediment from a locally irregular bed surface of the water tank, which will be disregarded in the following analysis.

Boulder Moving Feature

For all experiments, final block transport distance was recorded and summarized in Table 1. From the hydraulic experiments, it is confirmed that for Case I (90 degree), the concrete block was in general not dislodged under a $\Delta H=30$ cm condition, and was transported in cases of a $\Delta H=32$ or $\Delta H=35$ cm. Considering the moving process, block movement terminates at the location in accordance with a decreasing current velocity, i.e., around 0.9 m/s for both $\Delta H=32$ and $\Delta H=35$ cm. Considering Case II (45 degree), similar results were observed from the experiments (without/with block movement for $\Delta H=30/32, 35$ cm, respectively). In the Case II experiments, the block moving process was found in a swaying mode at the beginning stage, adjusting its orientation from the original 45 degree to 90 degree (perpendicular) to the current direction. Afterwards, block sustains its orientation (90 degree) until it comes to rest. This is in consistent with the experimental observation in Imamura et al. (2008). On the other hand, Imamura et al. claimed that the maximum block displacement for an initially current-block oblique setting was significantly shorter compared to those for the initially current-block perpendicular setting, which is because that part of the hydraulic force was used for rotating the block and the force available to transport the block becomes weaker. In our experiments for a $\Delta H=35$ cm, Case II

experiments resulted in a shorter transport distance (223.3 cm in average) than that of Case I experiments (232.5 cm in average), which agrees with Imamura et al. (2008). However, block displacements under a $\Delta H=32$ cm were found to be longer for Case II setting than its counterpart for Case I setting, even taking into account each individual test. This is ascribed to a larger projected area of the block against the current flow at the initial moving stage with respect to the Case II setting, which results a larger drag force acting on the block. The initial projected area is $\min(h(t) \times 22.63, 12 \times 22.63)$ cm² for the Case II setting, while it is $\min(h(t) \times 20, 12 \times 20)$ cm² for the Case I setting, in which $h(t)$ is the instantaneous water depth at the block position. As for the Case III experiments, there is no block movement for all considered initial water head settings, which is attributed to the small projected area ($12 \times 12 = 144$ cm²), and small drag force, under the Case III hydraulic setting.

Although the flow depth estimation required for boulder deposition, Goff et al. (2010) argued that the tsunami cannot realistically transport boulders in suspension, it limits the transport modes to bed load (sliding) or saltation. In our experiments except one test, the block was seen to be transported by a bore in a form of sliding, which is in consistent with the description of Walder et al. (2006) who concluded that block sliding is the preferred mode of block incipient motion. Noorments et al. (2004) also argued that sliding is a common mechanism of transport for larger and irregular megaclasts. In our experiments, the block is rather large in size with respect to the generated tsunami bores. As shown in Fig. 3, the maximum bore height measured at the initial block position is 13.31 cm for a $\Delta H=35$ cm, which is only 1.11 times of the block height (12 cm). When modeling the boulder movement, researchers generally assume the initial movement (dislodgment) of boulder in a form of sliding (Nott, 2003; Paris et al., 2010; Etienne et al., 2011) or rolling/overturning (Noorments et al., 2004; Etienne et al., 2011; Nandasena et al., 2011) considering the balance between the fluid forces or moments at the initial stage with either the resistance force for sliding or the resistance moments for overturning. Imamura et al. (2008) found that the cubic block was found to be transported mainly due to rolling or saltation rather than sliding in their experiments. This may be due to the relatively large ΔH (15-30 cm), which could induced a significant hydraulic forces to the used cubic block with a size of only 1.6-3.2 cm. Nevertheless, the block material they applied included the coral rock, which has a rather light density, 1.55-1.79 g/cm³, and facilitates the block movement in a rolling or saltation mode.

As for the only exception in our experiments (the third test for Case II with a $\Delta H=35$ cm), one time rolling was observed during the block movement. The rolling did not occurred at the beginning of the block motion, while the block rolled 90 degree in the middle of the moving process then slid till its rest. Imamura et al. (2008) argued that the bottom friction coefficient reduces with decrease in ground contact time when the block was transport by rolling or saltation, which lead to a longer transport distance than that of sliding transport mode. In our experiment, the final transport distance of this test was recorded as 214 cm, which is however shorter than the displacement from other two tests in sole sliding transport mode (229 and 227 cm in Table 1) under the same experimental conditions. This may be caused by the extra energy dissipation in accompany with the rolling process, and resulting in a weak hydraulic force exerting on the moving block afterwards.

BOULDER MOVING PROCESS

Measuring Technique

Previous studies, no matter field or laboratory ones, on the tsunami boulder movement focused on the total boulder displacement paying attention only to the initial and final locations of the boulder. There is no detailed information about the boulder moving process, e.g., the temporal boulder displacement and the moving velocity variation. However, such moving process could provide us the comprehensive physical insights on the tsunami boulder movement because the same total tsunami boulder displacements do not indicate the same incoming tsunami characteristics, e.g., tsunami height, current velocity and so on. Nevertheless, these tsunami features are crucial for assessing the historical tsunami scale and future disaster prevention/mitigation.

In this study, detailed block moving process was recorded using a video camera setting on the top of the water tank (Fig. 2). Consequently, the image analysis technique was applied to extract the time series of the instantaneous block position during its entire moving process. Considering the video camera was set at an oblique angle to the channel bed, a geometrical description of the camera position and orientation relative to the ground coordinate system is needed. Two-step image rectification was conducted to acquire the calibration parameters which link the accurate geo-referencing (the real world

coordinates) with the oblique video images (the image coordinate). The first step is to identify the camera internal calibration coefficients to remove the lens distortion (both radial and tangential), skewness coefficient and image principal point bias. Liu et al. (2012) method was applied in this study. The second step is to determine the camera external calibration coefficients. The geo-rectified image was generated based on the image rectification relationship proposed by Holland et al. (1997) with an improved accuracy after Liu et al. (2008), who introduced a weight function to the ground control points (GCP) to improve the accuracy of image rectification by enhancing the role of camera-far-field GCPs in the least-square analysis. After obtaining the time series of the geo-rectified images, detailed block moving process could be resolved. In this analysis, a time interval of 0.5 sec was applied for investigating the tsunami boulder moving process. Hereafter, only the Case I setting (normal tsunami incidence) was considered.

Boulder Displacement

Figure 5 shows the recorded temporal variation of the block displacement right after the bore reaches the block position under the $\Delta H=32$ cm and $\Delta H=35$ cm, respectively. Error bars (standard deviation) on data points indicate the variability from three experiments under the same experimental condition. The bore front arrival time of the block is set as zero in this figure. Considering a $\Delta H=32$ cm, the block starts and stops its movement 1 and 7 sec after the bore front hits the block, respectively, resulting in a total moving duration of 6 seconds and a transport distance of 115 cm. The block movement is not triggered immediately by the arrival of the water bore. Considering the block sliding transport mode in our experiment, the initial time lag of 1 sec indicates the bore-induced driving force exerting on the block is smaller than the resistance force during this period, which is owing to the temporally small water level at the block position. For instance, it takes 4 sec for the block to be completely submerged by the local water level (Fig. 3). With the increase of the water level, the drag force exerting on the block increases while the resistance force reduces due to the elevated buoyancy force. In contrast, Imamura et al. (2008) mentioned that in their hydraulic experiments, the block starts its movement simultaneously with the bore front hitting the block. This may be ascribed to the relatively high water level setting (water level to block size) and the light block material they used, which led to the block movement in a rolling or saltation mode as mentioned above. Yeh et al. (2005) mentioned that the tsunami forces acting on the structure include hydraulic force, buoyant force, hydrodynamic force, surge force, impact force and breaking wave force. Among which, the surge force plays an important role when considering the initial damage/failure of the structure. Our tests demonstrate all these forces together are not strong enough to make the block move instantly. As for a $\Delta H=35$ cm, the block is mobilized 0.5 seconds after the arrival of the tsunami bore and rests after 9 seconds. The final block displacement is 233 cm, two times of the $\Delta H=32$ cm case (although the ΔH difference is only 3 cm for these two cases). There is no significant difference on the temporal block displacement at the initial stage, i.e., before 3 sec; whereas, clear difference on block displacement could be easily identified after that.

Boulder Velocity

The time series of the block moving velocity is presented in Figure 6, which is estimated in terms of the recorded temporal block positions as shown in Fig. 5. In Fig. 6, it is seen that the block moving process can be specified into three different phases as highlighted using various arrows in the figure, i.e., the acceleration phase (1-2 sec for 32 cm case; 0-2.5 sec for 35 cm case), the deceleration phase (2-4 sec for 32 cm case; 2.5-4 sec for 35 cm case), and the relatively steady moving phase (4-7 sec for both 32 and 35 cm cases). Considering the physical features of the block moving velocity, there is no significant difference in the acceleration phase for the $\Delta H=32$ cm and $\Delta H=35$ cm. The maximum block moving velocity for these two cases is also the same, around 60 cm/s, which is about the half of the measured maximum bore velocity (~ 130 cm/s as shown in Fig. 4, paying attention that the bore velocity is measured at the $x=3$ m location). During the deceleration phase, a larger block moving velocity, in general, could be identified for the $\Delta H=35$ cm. Taking into account the instantaneous block displacement in Fig. 5, it could be recognized that difference on the temporal block displacement is mainly exaggerated from the deceleration phase. As for the steady moving phase, clear difference could be observed with the block moving velocity being about 8 cm/s for a $\Delta H=32$ cm, and being about 26 cm/s for a $\Delta H=35$ cm. This further differentiates the block displacement between these two settings. Accordingly, divergence on the block final displacements for these two cases is induced by the moving

velocity difference during the deceleration and steady moving phases. On the other hand and during the relatively steady block moving phase, the measured bore velocities at the $x=3$ m location as illustrated in Fig. 4 do not show the similar boulder moving steady feature (although in Fig. 4, there seems to be a sudden drop on the measured bore velocity at the time of 7 sec at which the block movement terminates). This experimental measurement/observation indicates the unsteady feature of the block moving process is not in completed accordance with the spatiotemporal variations of the water level and flow velocity. Boulder moving characteristics may vary from the temporal physical features of the bore propagation.

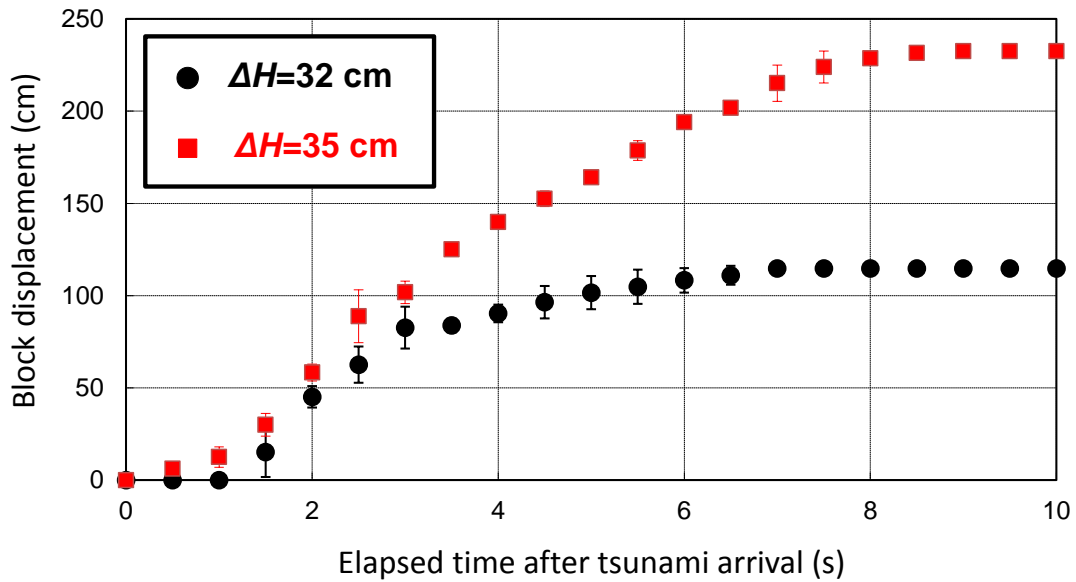


Figure 5. Temporal block displacement under the $\Delta H=32$ cm (●) and 35 cm (■) and normal incidence.

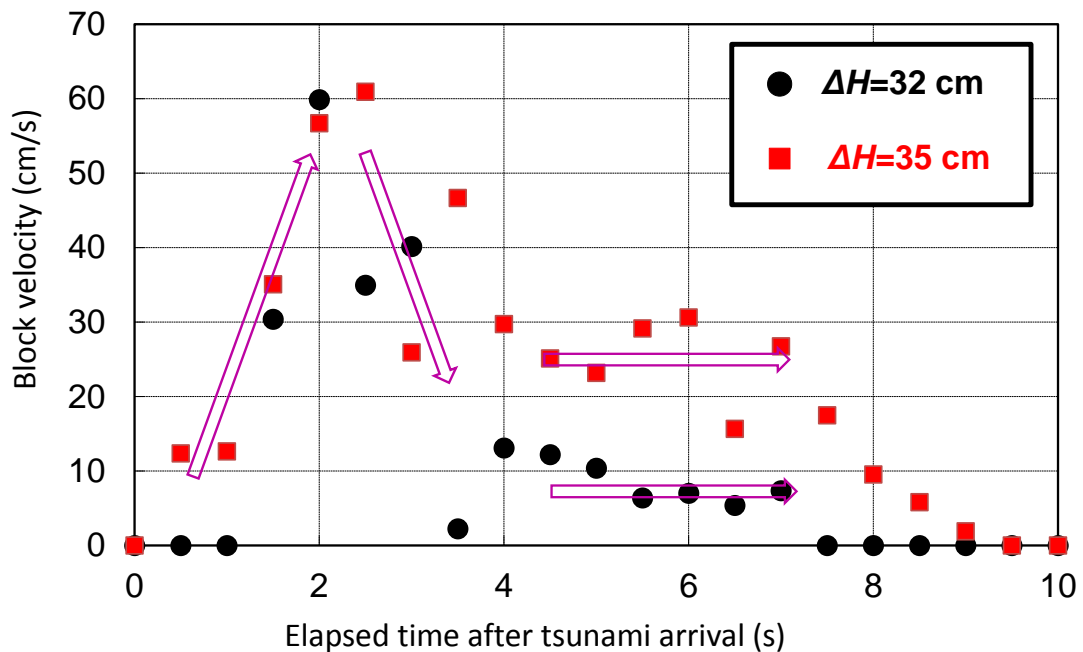


Figure 6. Temporal block moving velocity under the $\Delta H=32$ cm (●) and 35 cm (■) and normal incidence.

CONCLUSIONS

In this study, a series of dam-break type hydraulic experiments were conducted in an open channel with a concrete block setting on a horizontal bed just above the beach face to simulate the tsunami-induced boulder overland movement process, including the effect from the boulder orientation, moving type, instantaneous boulder displacement and velocity. The following conclusions can be drawn,

1. Sliding motion is the general mode for the large-sized tsunami boulder movement. A short boulder transport distance was confirmed for occasionally rolled boulder movement.
2. Comparing with the normal incident case, an oblique incident tsunami wave could lead to a longer boulder displacement owing to the large current-projected boulder area.
3. Instead of immediate dislodgement, boulder starts moving some time after the tsunami bore arrival.
4. A small change in the initial water head settings could lead to a significant difference on the total boulder displacement.
5. Three stages of the tsunami boulder moving process were confirmed from the physical experiment, i.e., the acceleration phase, the deceleration phase and the relatively steady moving phase.
6. The variation on the total boulder displacement is mainly ascribed to the boulder moving velocity difference during the deceleration and steady moving phases.
7. This experimental measurement/observation indicates the unsteady feature of the tsunami boulder moving process is not in completed accordance with the spatiotemporal variations of the water level and bore propagating velocity.

ACKNOWLEDGEMENTS

Acknowledgement goes to Prof. A. Okayasu and Dr. T. Shimozone for allowing us to use the water tank facility at Tokyo University of Marine Science and Technology. HL was supported by the fundamental research funds for the central universities (No. 2013QNA4039), and the Natural Science Foundation of Zhejiang Province (No. LR14E090002).

REFERENCES

- Bryant, E.A., Young, R.W., Price, D.M., 1992. Evidence of tsunami sedimentation on the Southeastern Coast of Australia. *Journal of Geology*, 100, 753–765.
- Costa, P.J.M., Andrade, C., Freitas, M.C., Oliveira, M.A., da Silva, C.M., Omira, R., Taborda, R., Baptista, M.A., Dawson, A.G., 2011. Boulder deposition Turing major tsunami events. *Earth Surf. Process. Landforms*, 36, 2054-2068.
- Dawson, A.G., Shi, S., 2000. Tsunami deposits. *Pure Appl. Geophys.*, 157, 875-897.
- Etienne, S., Buckley, M., Paris, R., Nandasena, A.K., Clark, K., Strotz, L., Chagué-Goff, C., Goff, J., Richmond, B., 2011. The use of boulders for characterizing past tsunamis: Lessons from the 2004 Indian Ocean and 2009 South Pacific tsunamis. *Earth-Science Reviews*, 107, 76-90.
- Frohlich, C., Hornbach, M.J., Taylor, F.W., Shen, C.-C., Moala A., Morton, A.E., Kruger, J., 2009. Huge erratic boulders in Tonga deposited by a prehistoric tsunami. *Geology*, 37(2), 131-134.
- Goff, J., Dudley, W.C., Maintenon, M.J., Cain, G., Coney, J.P., 2006. The largest local tsunami in 20th century Hawaii. *Marine Geology*, 226, 65–79.
- Goff, J., Weiss, R., Courtney, C., Dominey-Howes, D., 2010. Testing the hypothesis for tsunami boulder deposition from suspension. *Marine Geology*, 277, 73-77.
- Goto, K., Chavanich, S.A., Imamura, F., Kunthasap, P., Matsui, T., Minoura, K., Sugawara, D., Yanagisawa, H., 2007. Distribution, origin and transport process of boulders deposited by the 2004 Indian Ocean tsunami at Pakarang Cape, Thailand. *Sedimentary Geology*, 202, 821-837.
- Goto, K., Okada, K., Imamura, F., 2010. Numerical analysis of boulder transport by the 2004 Indian Ocean tsunami at Pakarang Cape, Thailand. *Marine Geology*, 268, 97–105.
- Hall, A.M., Hansom, J.D., Williams, D.M., 2010. Wave-emplaced coarse debris and megaclasts in Ireland and Scotland: boulder transport in high-energy littoral environment: a discussion. *Journal of Geology*, 118, 699–704.
- Hearty, P.J., 1997. Boulder deposits from large waves during the last interglaciation on North Eleuthera Island, Bahamas. *Quaternary Research*, 48, 326–338.
- Holland, K.T., R.A. Holman, T.C. Lippmann, and J. Stanley. 1997. Practical use of video imagery in nearshore oceanographic field studies. *IEEE J. of Oceanic Eng.*, 22(1), 81-92.

- Imamura, F., Goto, K., Ohkubo, S., 2008. A numerical model for the transport of a boulder by tsunami. *Journal of Geophysical Research*, 113, C01008.
- Kato, Y., Kimura, M., 1983. Age and origin of so-called "Tsunami-ishi", Ishigaki island, Okinawa prefecture. *J. Geol. Soc. Japan*, 89, 471-474.
- Liu, H., Y. Tajima, and S. Sato. 2008. Field study on the nearshore sediment process around the Tenryu estuary using image analysis, *Proceedings of 31st International Conference on Coastal Engineering*, Hamburg, Germany, 2064-2076.
- Liu, H., Arii, M., Sato, S., Tajima, Y., 2012. Long-term nearshore bathymetry evolution from video imagery: a case study in the Miyazaki coast. *Proceedings of 33rd International Conference on Coastal Engineering*, Santander, Spain, doi:10.9753/icce.v33.sediment.60.
- Liu, H., Shimozono, T., Takagawa, T., Okayasu, A., Fritz, H.M., Sato, S., Tajima, Y. (2013). The 11 March 2011 Tohoku tsunami survey in Rikuzentakata and a historical review. *Pure Appl. Geophys.*, doi: 10.1007/s00024-012-0496-2, 170(6), 1033-1046.
- Mastronuzzi, G., Sansò, P., 2000. Boulders transport by catastrophic waves along the Ionian coast of Apulia (southern Italy). *Marine Geology*, 170, 93-103.
- Nandasena, N.A.K., Paris, R., Tanaka, N., 2011. Numerical assessment of boulder transport by the 2004 Indian Ocean tsunami in Lhok Nga, West Bandah Aceh (Sumatra, Indonesia). *Computers and Geosciences*, 37, 1391-1399.
- Noji, M., Imamura, F., Shuto, N., 1993. Numerical simulation of movement of large rocks transported by tsunamis. *Proceedings of IUGG/IOC International Tsunami Symposium*, 189-197.
- Noormets, R., Crook, K.A.W., Felton, E.A., 2004. Sedimentology of rocky shorelines: 3. Hydrodynamics of megaclast emplacement and transport on a shore platform, Oahu, Hawaii. *Sedimentary Geology*, 172, 41-65.
- Nott, J., 2003. Waves, coastal boulder deposits and the importance of the pre-transport setting. *Earth and Planetary Science Letters*, 210, 269-276.
- Nott, J., Bryant, E., 2003. Extreme marine inundations (tsunamis?) of coastal Western Australia. *Journal of Geology*, 111, 691-706.
- Paris, R., Fournier, J., Poizot, E., Etienne, S., Morin, J., Lavigne, F., Wassmer, P., 2010. Boulder and fine sediment transport and deposition by the 2004 tsunami in Lhok Nga (western Banda Aceh, Sumatra, Indonesia): A coupled offshore-onshore model. *Marine Geology*, 268, 43-54.
- Pignatelli, C., Sansò, P., Mastronuzzi, G., 2009. Evaluation of tsunami flooding using geomorphologic evidence. *Marine Geology* 260, 6-18.
- Ramsden, J.D., 1993. *Tsunamis: forces on a vertical wall caused by long waves, bores, and surges on a dry bed*. Ph.D. Dissertation, California Institute of Technology, pp251.
- Razzhigaeva, N.G., Ganzei, L.A., Grebennikova, T.A., Ivanova, E.D., Kaistrenko, V.M., 2006. Sedimentation particularities during the tsunami of December 26, 2004, in Northern Indonesia: Simelue Island and the Medan Coast of Sumatra Island. *Oceanology*, 46(6), 875-890.
- Sato, S., Liu, H., Takewaka, S., Nobuoka, H., Aoki, S., 2012. Tsunami damages of Nakoso Coast due to the 2011 Tohoku Earthquake. *Proceedings of 33rd International Conference on Coastal Engineering*, Santander, Spain, doi:10.9753/icce.v33.currents.2.
- Scheffers, A., Kelletat, D., 2003. Sedimentologic and geomorphologic tsunami imprints worldwide – a review. *Earth-Science Reviews*, 63, 83-92.
- Scheffers, A., Scheffers, S., Kelletat, D., Browne, T., 2009. Wave-emplaced coarse debris and megaclasts in Ireland and Scotland: boulder transport in high-energy littoral environment. *Journal of Geology*, 117, 553-573.
- Scicchitano, G., Monaco, C., Tortorici, L., 2007. Large boulder deposits by tsunami waves along the Ionian coast of south-eastern Sicily (Italy). *Marine Geology*, 238, 75-91.
- Shi, S., Dawson, A.G., Smith, D.E., 1995. Coastal sedimentation associated with the December 12th, 1992 tsunami in Flores, Indonesia. *Pure Appl. Geophys.*, 144, 525-536.
- Switzer, A.D., Burston, J.M., 2010. Competing mechanisms for boulder deposition on the southeast Australian coast. *Geomorphology*, 114, 42-54.
- Walder, J. S., Watts, P., Waythomas, C. G. (2006). Case study: Mapping tsunami hazards associated with debris flow into a reservoir. *J. Hydraul. Eng.*, ASCE, 132, 1-11.
- Yeh, H., Robertson, I., Preuss, J., 2005. *Development of design guidelines for structures that serve as tsunami vertical evacuation sites*. Division of Geology and earth Resources, Open file Report 2005-4, Washington State of Department of Natural Resources, pp 34.